CryoLetters **42 (2)**, 96 – 105 (2021)

CRYO-RADIOFREQUENCY STIMULATES BROWNING OF ADIPOCYTES IN MICE

Marina Chaves de Oliveira[1,#], Amanda Carla Clemente de Oliveira[1,#], Daibes Lisboa[2], Graziele Maia Alves Serafim[2], Ana Letícia Malheiros Silveira[1] and Adaliene Versiani Matos Ferreira[1,*]

[1]Department of Nutrition, Nursing School, Universidade Federal de Minas Gerais, Belo Horizonte, Minas Gerais, Brazil.
[2]Body Health Brasil, Sete Lagoas, Minas Gerais, Brazil.
[#] Equal contributors; *Corresponding author's E-mail: adaliene@gmail.com

Abstract

BACKGROUND: Local fat accumulation is a health risk and this has raised interest in the development of aesthetic treatments, such as cryo-radiofrequency (CRF). **OBJECTIVE:** To evaluate the consequences of CRF in adipose tissue remodeling in a model system. **MATERIALS AND METHODS:** Lean and high-fat diet-induced obese mice were assessed 7 days after one CRF application; and lean mice were assessed 0, 3, 6 and 12 h after one application of CRF. Assessments included histology, DNA degradation, gene expression, ELISA of cytokines, serum analysis and neutrophil presence. **RESULTS:** Unchanged fat mass was found 7 days after CRF in obese and lean mice. However, lean mice showed smaller adipocyte size with areas resembling a browning process. TNF levels, apoptotic cells, and UCP-1 expression increased 7 days after CRF in inguinal adipose tissue of lean mice. Although no differences were found in fat mass, adipocyte size decreased just after CRF and this changed was maintained until 12 h, with cells resembling beige adipocytes. **CONCLUSION:** We suggest that CRF therapy is capable of inducing thermogenic adipocytes in lean mice.

Keywords: adipose tissue; browning; cryo-radiofrequency (CRF); obesity.

INTRODUCTION

Adipose tissue is an essential metabolic and endocrine organ involved with the regulation of energetic metabolism, immune response, and thermogenesis (1). Two different types of adipose tissue are known: white and brown. Both tissues store triglycerides in adipocytes, but those of brown adipose tissue also have a considerable number of mitochondria with a higher expression of uncoupling protein 1 (UCP-1) (2). UCP-1 is essential for the heat production process and is mainly regulated by fatty acids, which, in turn, are the primary substrates for oxidation during thermogenesis (3). Recently, it has been shown that adipocytes present in the middle of white adipose tissue could also express UCP-1 when adequately activated. Thus, it has been called a new type of fat tissue, the beige adipose tissue. The differentiation of beige rather than white adipocytes has been described as browning (4, 5). Chronic adrenergic activation in cold-exposed rodents leads to the development of beige adipocytes in white adipose tissues (6), which contributes to their thermogenic function. Thus, brown adipose tissue, as well as the beige type, have become potential targets in the investigation of possible treatments related to obesity and other associated comorbidities.

Obesity is a disease characterized by adipose tissue expansion and chronic low-grade inflammation (7). Recently, the prevalence of obesity has increased in lower-middle to high-

income countries (8), pointing out the necessity for the development of useful treatment options. In this sense, multiple ways to reduce fat mass have been developed that include food intake control, central nervous system regulation, energy expenditure, endocrine system regulation, and direct fatty tissue removal (9, 10). However, few methods have succeeded in effectively reducing localized fat pad mass. In this sense, new aesthetic machinery has been proposed to help to reduce local fat accumulation (11-15). Among them, radiofrequency has shown positive effects on the reduction of local adipose tissue in clinical practice (16-18). The radiofrequency (RF) is a form of high-frequency electromagnetic energy that works by heating the tissues, acting on deeper layers of the skin and subcutaneous tissue to raise cellular metabolism (19). New equipment developed combines the transmission of cold from the handle to the dermis, with internal heating of body tissues caused by the multipolar radiofrequency waves, the cryo-radiofrequency (CRF). As thermogenesis may be induced by cold and the effects of this therapy on adipose tissue have not yet been described, we aimed to evaluate whether the cryo-radiofrequency therapy could contribute with adipose tissue remodeling in obesity.

Herein, we show that CRF stimulates the browning of white adipocytes that may change the adipose tissue morphology in lean mice. We also showed that in obese mice, one application of CRF was not enough to alter the tissue morphology showing that this treatment may be more efficient at changing fat metabolism locally.

MATERIALS AND METHODS

Animals and diets

Female BALB/c mice were provided by the Bioterium Center of the Universidade Federal de Minas Gerais (UFMG). They were maintained in a controlled environment with a 12 h: 12 h light: dark cycle, and in collective cages with *ad libitum* access to food and water. The experiments were approved by the "Ethics Committee for Animal Experimentation of the UFMG" (protocol number: 201 / 2018).

Female mice at 8 weeks of age were randomly divided into two groups and received the following diets: chow as a control group (C) and the high-fat (HF) diet for eight weeks to induce obesity. The nutrient composition of chow diet (4.0 kcal/g) was 65.8% of weight as carbohydrate, 3.1% as fat, and 31.1% as protein; the HF diet (7.0 kcal/g) was 24.5% of weight as carbohydrate, 61.0% as fat, and 14.5% as protein. The lipid content of the HF diet was mostly composed of lard. After this period, mice underwent one application of cryo-radiofrequency (CRF) and seven days after that were killed. Body-weight gain was measured once a week, and the food intake was measured twice a week. In another set of experiments, female mice at 20 weeks of age were divided into five different groups: (i) CRF equipment off, and mice killed (ii) 0 h, (iii) 3 h, (iv) 6 h or (v) 12 h after one CRF application.

Blood was collected from the tail vein of mice and total white blood cells were counted using a Neubauer chamber. Samples of blood, visceral (perigonadal, retroperitoneal and mesenteric) and subcutaneous (inguinal) adipose tissues were collected for further analyses. The adiposity index was calculated as a percentage of the weights of perigonadal, retroperitoneal, mesenteric and inguinal adipose tissues to the body mass.

Cryo-radiofrequency (CRF) therapy

CRF sessions were performed using BHS 156 equipment (Body Health Brazil, Sete Lagoas, Brazil). This equipment combines the transmission of cold (-25°C) from the handle to the dermis, with internal heating of body tissues (over 55°C) caused by the multipolar radiofrequency waves. Animals were anesthetized with intraperitoneal injection at a dose of 4.5 mL / kg xylazine hydrochloride solution (10 mg / kg) and ketamine hydrochloride (80 mg / kg) diluted in 0.9% NaCl. Mice were embedded in a gel to avoid the occurrence of shocks. The equipment was turned on and adjusted to a power of 85 watts. Then the animals were subjected to a light massage with monopolar CRF waves in the abdominal region with the tip of the equipment for 4 min, and the temperature was around -6°C. In the control group, the same procedure was performed but with no CRF application. After that, they were placed on a warm plate until they return from anesthesia.

Intravital microscopy

The intravital microscopy was performed as previously described (20). Briefly, after the CRF session and the determined period, mice

were anesthetized by i.p. injection of 130 mg/kg ketamine and 0.3 mg/kg xylazine. In the perigonadal adipose tissue, the number of leukocytes rolling, and adhered to the vascular wall was evaluated. Leukocytes were fluorescently labeled by i.v. administration of rhodamine 6G (1.5 mg/kg body weight; Sigma, St. Louis, MO) and observed on a fluorescence microscope (Nikon H550L, 20x objective lenses). Rolling leukocytes were defined as cells passing through an imaginary transverse line to the vessel for 60 s and moving at a velocity less than that of erythrocytes. Leukocytes were considered adherent to the venular endothelium whether they remained stationary for a period of 30 s or longer in a vessel fragment of approximately 100 µm. The two parameters were measured in two or three different vessels and averaged for each animal.

Histological analyses

Samples of perigonadal and inguinal adipose tissues were fixated in formaldehyde 4% for 48 h, dehydrated and embedded in paraffin. Sections of tissue were stained with hematoxylin-eosin (H&E). Images of six fields from adipose tissue of each animal were captured using a digital camera coupled to a microscope (100x) using Image Pro-Plus software (Media Cybernetics, USA) to determine adipocyte area. The area of 50 adipocytes was measured in each animal by ImageJ (National Institutes of Health, Bethesda, Maryland, USA) to calculate the mean adipocyte area (μm^2) (21).

Tunel staining

The TUNEL staining was performed with the DNA fragmentation detection kit TdT-FragEL (EMD Biosciences, San Diego, CA), following the manufacturer's instructions. Images of five fields from adipose tissue of each animal were captured using a digital camera coupled to a microscope (100X) using Image Pro-Plus software (Media Cybernetics, USA) to quantify apoptotic cells. The number of apoptotic cells in each animal was calculated as the total amount of cells counted in all fields divided by the number of fields.

The enzyme-linked immunosorbent assay (ELISA)

DuoSet ELISA kits measured TNF-α and IL-10 cytokines in perigonadal and inguinal adipose tissues according to the instructions provided by the manufacturer (R&D System, Inc., Minneapolis, USA).

Serum analyses

Glucose, triglyceride and total cholesterol serum levels were measured by enzymatic kits (Bioclin, Belo Horizonte, Brazil). Leptin, adiponectin and resistin levels were analyzed in serum using a DuoSet ELISA kit (R&D System, Inc., Minneapolis, USA) according to the manufacturer's instruction.

qPCR analysis

Total RNA from inguinal adipose tissue was extracted using the Aurum total RNA mini kit (BioRad, California, USA) and the samples were treated with DNAse as suggested by the manufacturer. The purity of RNA was checked spectrophotometrically, and the reverse transcription was carried out using the iScript cDNA synthesis kit (BioRad, California, USA). The real-time polymerase chain reaction (PCR) was performed using the SYBR Green PCR Master Mix (Applied Biosystems) on an ABI PRISM 7500 sequence-detection system (Applied Biosystems, Warrington, UK). The relative gene expression of *Ucp1* (uncoupling protein 1) and *Pgc1α* (peroxisome proliferator-activated receptor γ coactivator 1α) was assessed, determined by the $2^{-(\Delta\Delta Ct)}$ method, and normalized by the housekeeping ribosomal 18S expression. The following primer pairs, designated as forward (For) and reverse (Rev) for the investigated RNA sequences, were utilized: (i) *Ucp1* For: 5'- ACC CGA GTC GCA GAA AAG AAG-3'; *Ucp1* Rev: 5'- CGA TGT CCA TGT ACA CCA AGG A- 3'; (ii) *Pgc1α* For: 5'- GGA GCC GTG ACC ACT GAC A-3'; *Pgc1α* Rev: 5'- TGG TTT CGT GCA TGG TTC TG-3'.

Myeloperoxidase (MPO) and N-acetyl glucosaminidase (NAG) activity

The indirect neutrophil presence was measured by assaying MPO activity, as described previously (22). Briefly, perigonadal and inguinal adipose tissue samples were homogenized and assayed for MPO activity by measuring the change in OD at 450 nm using tetramethylbenzidine.

The relative numbers of macrophages in the perigonadal and inguinal adipose tissues were quantified by measuring the NAG activity. Briefly, a portion of these tissues was homogenized and centrifuged at 4°C for 10 min at 3,000 rpm. The supernatants were collected

and assayed immediately for NAG activity, as described previously (23).

Statistical analyses

Results were expressed as means ± SEM and analyzed using GraphPad Prism version 5.0 (GraphPad Software, San Diego, CA). All data were analyzed for normality of distribution using the Kolmogorov-Smirnov test and were found to be normal. Comparison between two groups was performed using Student's t-test. Comparisons between more than two groups were performed using one way analysis of variance (ANOVA) followed by the post hoc test of the Dunnett or Newman-Keuls. Statistical significance was set at $P < 0.05$.

RESULTS

A CRF application was performed, and after 7 days mice were killed to analyze the effect of CRF on adipose tissue of lean and obese mice. First, obesity in mice as induced by a change in diet for 8 weeks. As expected, mice fed with HF diet presented increased body weight gain (Figure 1a) and feeding efficiency (C = 14.33 ± 3.012 g/Kcal and HF = 22.08 ± 5.28 g/Kcal; $P<0.05$) compared to mice fed with chow diet. This increased weight was associated with a higher amount of visceral adipose tissues, as perigonadal, retroperitoneal and mesenteric,

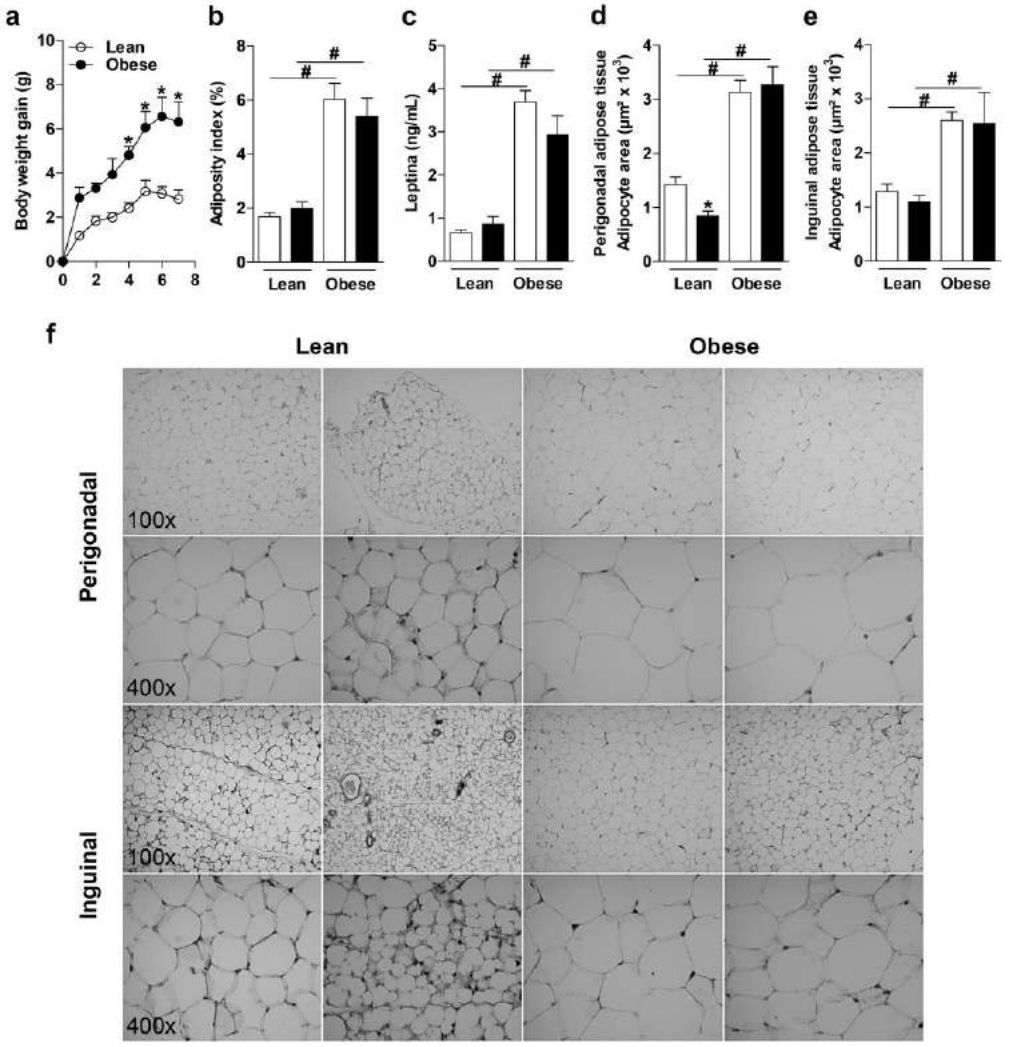

Figure 1. Adipose tissue alterations of mice submitted to the cryo-radiofrequency (CRF) application in lean and obese mice. (a) Body weight gain of lean fed with chow diet and obese mice fed with high-fat (HF) diet. (b) Adipocyte index (percentage of the weights of perigonadal, retroperitoneal, mesenteric and inguinal adipose tissues to the body mass). (c) Leptin serum levels. Adipocyte area of (d) perigonadal adipose tissue and (e) inguinal adipose tissue. (f) Representative images of adipose tissue histology of mice with no CRF application (control) or 7 days (7 d) after application of CRF; for lean and obese, the controls and treatments are shown in left and right pairs. Bars are means (n=5-8) ± SE. **P*<0.05 compared with control and #*P*<0.05 compared with obese by one-way ANOVA post hoc Neuman-Keuls test.

Table 1. Metabolic parameters of mice 7 days after one application of cryo-radiofrequency.

Parameters	Lean Mean ± SEM	Lean + CRF Mean ± SEM	*P*-value
Glucose (mmol/L)	10.0 ± 0.51	10.5 ± 0.14	0.3032
Triglycerides (mmol/L)	2.4 ± 0.14	2.6 ± 0.33	0.5230
Total cholesterol (mmol/L)	2.4 ± 0.29	2.9 ± 0.09	0.0690
Adiponectin (µg/ml)	6.1 ± 0.26	6.0 ± 0.10	0.7694
Resistin (ng/ml)	19.2 ± 4.84	14.6 ± 2.95	0.4069

CRF: cryo-radiofrequency; SEM: standard error of the mean.
Statistically analyzed by Student's t-test (n = 5-8).

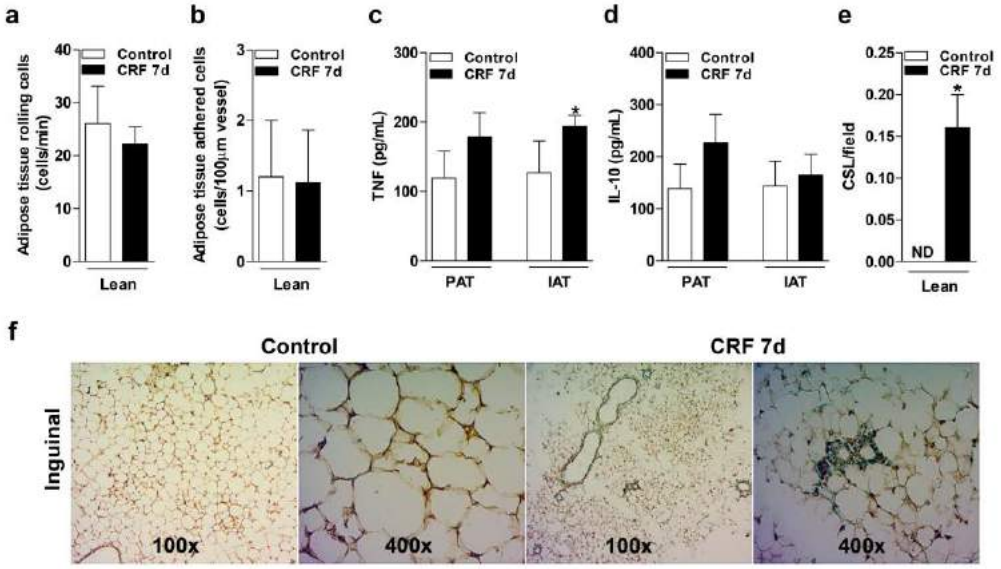

Figure 2. (a) Rolling and (b) adhered leukocytes in the perigonadal adipose tissue of mice submitted to the cryo-radiofrequency (CRF) application. (c) Tumor necrosis factor (TNF) levels in perigonadal adipose tissue (PAT) and inguinal adipose tissue (IAT). (d) Interleukin-10 (IL-10) levels in perigonadal adipose tissue (PAT) and inguinal adipose tissue (IAT). Histological analysis of apoptotic cells from inguinal adipose tissue: (e) Number of apoptotic cells per field and (f) representative images of apoptotic cells of lean mice with no CRF application (control) or 7 days (7d) after application of CRF. The bars represent the mean values ± standard error of the mean (n=5-8). **P*<0.05 by Student's t-test vs. control.

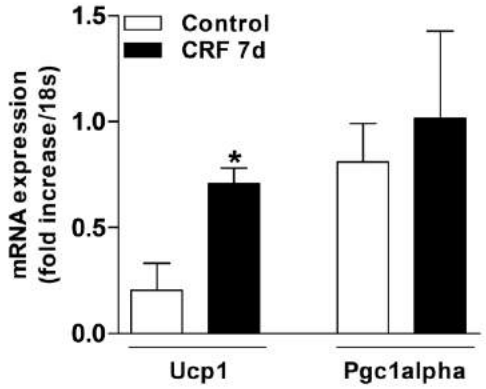

Figure 3. Browning in inguinal adipose tissue of lean mice submitted to the cryo-radiofrequency (CRF) application. UCP1 and PGC1α of lean mice with no CRF application (control) or 7 days (7d) after application of CRF. The bars represent the mean values ± standard error of the mean (n=5-8). **P*<0.05 by Student's t-test vs. control

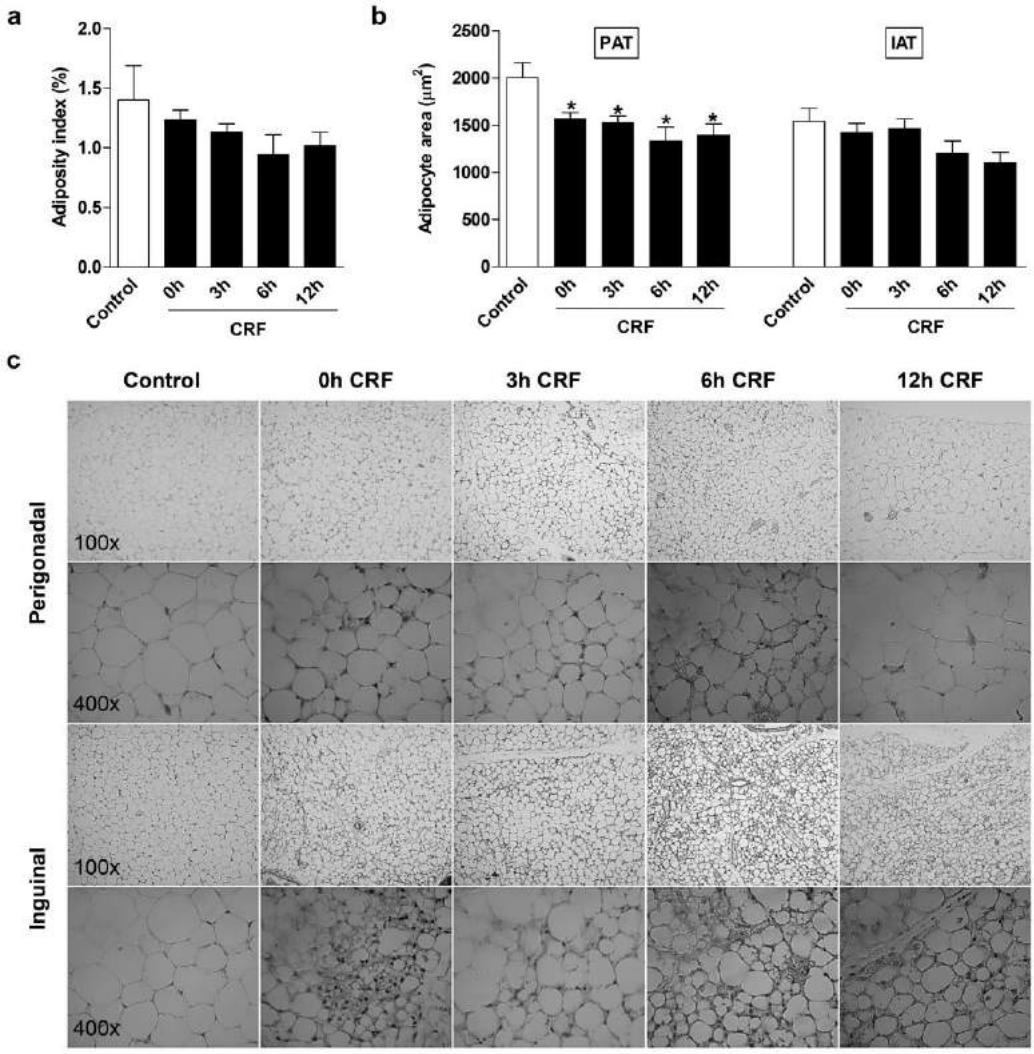

Figure 4. Adipose tissue alterations of mice submitted to the cryo-radiofrequency (CRF) application. (a) Adipocyte index (percentage of the weights of perigonadal, retroperitoneal, mesenteric and inguinal adipose tissues to the body mass). Adipocyte area of (b) perigonadal adipose tissue (PAT) and inguinal adipose tissue (IAT). (c) Representative images of adipose tissue histology of lean mice with no CRF application (control) or 0, 3, 6 and 12 h after application of CRF. The bars represent the mean values ± standard error of the mean (n = 5-6). *P<0.05 by one-way ANOVA post hoc Dunnett test vs. control.

and subcutaneous, as inguinal represented by adiposity index (Figure 1b). After 7 days of CRF application, both lean and obese mice did not show alterations in adipose tissue mass (Figure 1b). Consistently with the increased adiposity, serum leptin levels were increased in mice fed with the HF diet. No changes were observed in mice after the CRF application (Figure 1c). Mice fed with the HF diet showed increased perigonadal and inguinal adipocyte area. One application of CRF reduced the mean adipocyte area of lean mice, but not in obese (Figure 1d, e, f). In agreement with that, lean mice on day 7 after radiofrequency showed alterations in the characteristics of adipose tissue morphology, as observed in the representative images of the tissue (Figure 1f).

Because adipose tissue morphology was altered in lean mice after 7 d of a CRF session, metabolic and inflammatory analyses were performed in the serum and adipose tissue only in these groups. No alterations in glucose, triglycerides, total cholesterol, adiponectin and resistin serum levels were observed in lean mice

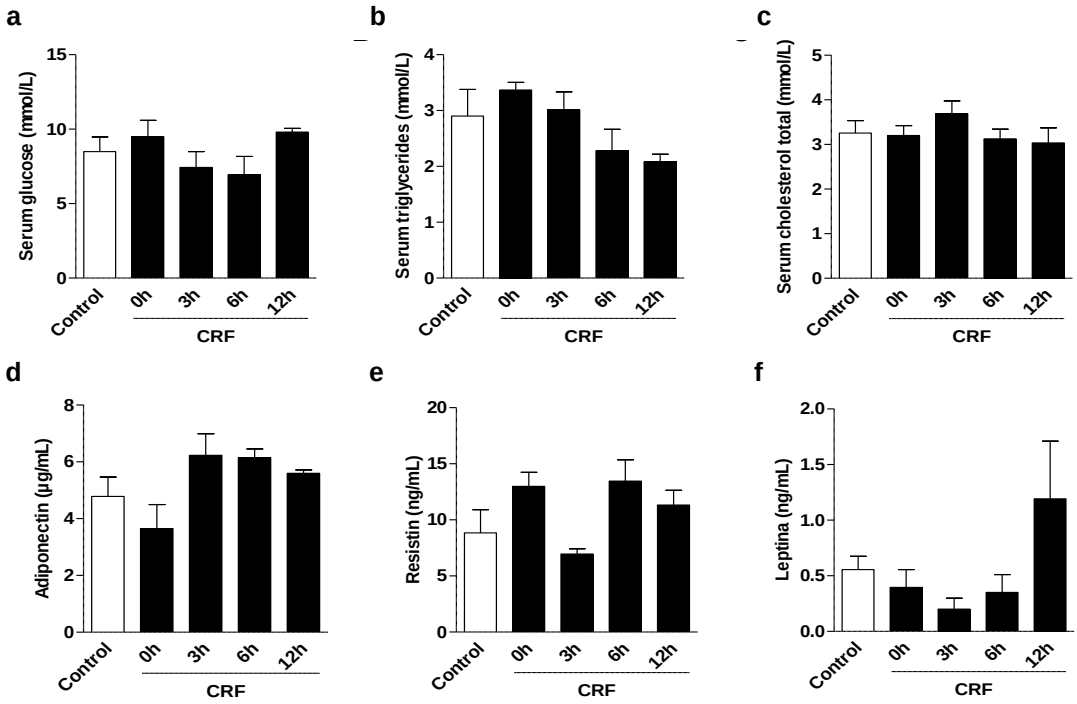

Figure 5. Glucose, lipid and adipokine levels in the serum of mice submitted to the cryo-radiofrequency (CRF) application. Serum (a) glucose, (b) triglycerides, (c) total cholesterol, (d) adiponectin, (e) resistin, and (f) leptin of lean mice with no application (control) or 0, 3, 6 and 12 h after application of CRF. The bars represent the mean values ± standard error of the mean (n = 5-6). $P<0.05$ by one-way ANOVA post hoc Dunnett test vs. control.

7 d after one application of CRF (Table 1). CRF did not change the number of leukocyte cells in the blood (Control = 10.2 x 10^7 ± 1.6 cells and CRF7d = 8.4 x 10^7 ± 1.2 cells; $P<0.05$). Accordingly, the CRF procedure did not change the rolling (Figure 2a) and adhering (Figure 2b) of leukocytes in perigonadal vessels of adipose tissue. No changes in TNF-α and IL-10 were found in perigonadal adipose tissues 7 d after CRF (Figure 2c and 2d). Although the amount of IL-10 in inguinal adipose tissue did not alter (Figure 2d), the concentrations of TNF-α (Figure 2c) and the number of apoptotic cells in the subcutaneous adipose tissue were higher (Figure 2e and 2f) in those that received the CRF application. Then, the expression of UCP-1 and PGC1α was evaluated in inguinal adipose tissue to exploring the capacity of this altered tissue morphology caused by CRF application. Higher UCP-1 expression was observed 7 d after one application of CRF. No changes were found in PGC1α expression (Figure 3).

After one application of CRF, lean mice were killed at 0, 3, 6 and 12 h to check the acute effect of this equipment on adipose tissue, inflammation, and metabolism. Although no alteration in adiposity index was observed after CRF at 0, 3, 6 and 12 h after one application (Figure 4a), a reduction in adipocyte area was seen in the perigonadal adipose tissue in all-time points evaluated, but not in the inguinal adipose tissue (Figure 4b). Interestingly, both tissues presented in the representative images of adipocytes an alteration in their morphology (Figure 4c). In the analysis of metabolism and adipokines, the serum levels of glucose, triglycerides, total cholesterol, adiponectin, resistin, and leptin showed no alteration after one application of CRF in the different time points analyzed (Figure 5). Besides, the analyses of cytokine levels of TNF and IL-10 in the perigonadal and inguinal adipose tissues, in general, did not present any alteration (Figure 6) as well as for MPO and NAG activity in both tissues (Figure 7). Only a reduction of IL-10 levels at 12 h after CRF was observed in inguinal adipose tissue compared with the control group (Figure 6d).

DISCUSSION

The investigation of new therapies that contribute to adipose tissue remodeling and the formation of beige adipocytes has increased in

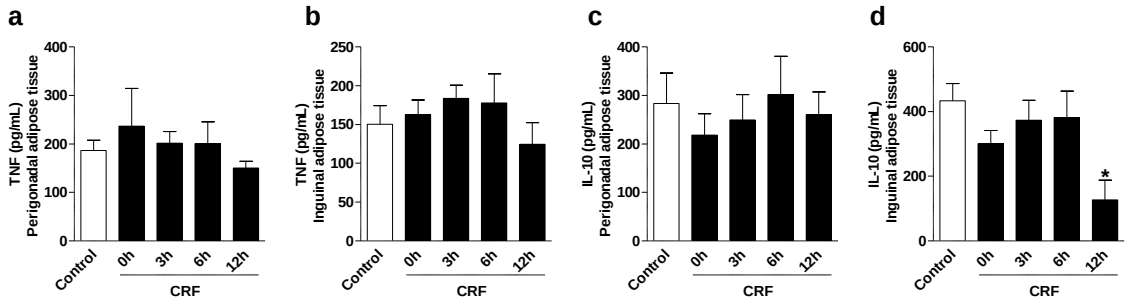

Figure 6. Cytokine levels in perigonadal adipose tissue and inguinal adipose tissue of mice submitted to the cryo-radiofrequency (CRF) application. Tumor necrosis factor (TNF) levels in (a) perigonadal adipose tissue and (b) inguinal adipose tissue. Interleukin-10 (IL-10) levels in (c) perigonadal adipose tissue and (d) inguinal adipose tissue of lean mice with no CRF application (control) or 0, 3, 6 and 12 h after application of CRF. The bars represent the mean values ± standard error of the mean (n = 5-6). **P*<0.05 by one-way ANOVA post hoc Dunnett test vs. control.

the last few years (4, 24, 25). The significant points of this study were: (i) a CRF application induces an acute alteration in the morphology of adipose tissue without metabolic and inflammatory alterations; (ii) adipose tissue of lean mice 7 d after one application of CRF changes the adipocyte morphology with an increase in apoptotic cells and UCP-1 expression; and (iii) adipose tissue of mice fed with the HF diet is not altered 7 d after one CRF application.

Obesity is a disease with increasing prevalence defined by higher fat mass that can alter or not the body weight and contribute to metabolic complications (26). In the last decades, the interest for strategies to reduce fat mass, such as dietary intervention or aesthetic treatments as liposuction, radiofrequency, and CRF has increased (11). Liposuction is the most performed cosmetic procedure, which consists of a surgical removing of fat deposits, improving body contours and proportion (12). Radiofrequency, on the other hand, is a non-invasive procedure which also improves the body contours by decreasing the abdominal circumference and adipose tissue thickness in the abdominal region of women (13-15). Similar to humans, this treatment also reduces body weight and fat deposits in obese mice (25).

Radiofrequency is a treatment that generates heat by producing an electrical current through an electromagnetic spectrum with frequencies from 3 kHz to 300 MHz (27). The heat produced by radiofrequency is supposed to change or disrupt the structure of adipocytes, which stimulates the secretion of TNFα, inducing lipolysis (28). The free fatty acids produced by lipolysis recruit and activate immune cell-like macrophages that maintain a pro-inflammatory environment and reduces the adipocyte size and, consequently, the fat mass (29). The intensification of this process disrupts

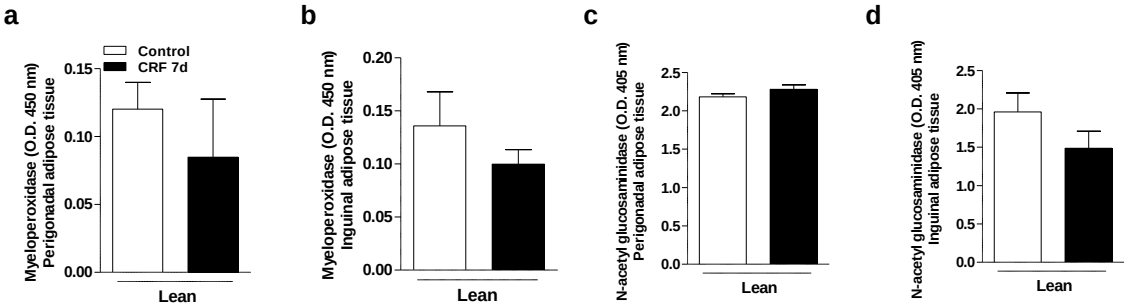

Figure 7. Indirect measurement of neutrophils by myeloperoxidase activity (MPO) in (a) perigonadal and (b) inguinal adipose tissues or macrophages by N-acetyl glucosaminidase (NAG) in (c) perigonadal and (d) inguinal adipose tissues of lean mice with no cryo-radiofrequency (CRF) application (control) or 7 days (7d) after application of CRF. The bars represent the mean values ± standard error of the mean (n=5-8). Statistical analysis by Student's t-test (P>0,05 vs. control).

the adipocyte membrane, causing cell death (30, 31).

Herein we analyzed the effect of one application of CRF in lean and obese mice. We showed that one application of CRF did not reduce the body weight or fat deposits in obese mice. However, one application of CRF was able to change the morphology of adipose tissue of lean mice. Thus, after that, we performed temporal analyzes to check the effect of CRF on local adiposity of lean mice. We showed that one application of CRF after 0, 3, 6, and 12 h was capable of reducing the adipocyte area of perigonadal adipose tissue. However, a smaller adipocyte size was not accompanied by significant inflammatory changes in this tissue. We also showed higher concentrations of TNF and a higher number of apoptotic cells in mice with CRF application in inguinal adipose tissue. McDaniel et al. (2014) showed that after four applications of radiofrequency with cooling in swine increased apoptotic cells in subcutaneous adipose tissue (32). CRF combines the production of heat with cooling, explaining partially our data. Although our protocol with one application of CRF did not reduce the mice's fat mass, it was enough to elevate the amount of TNF and apoptotic cells in the subcutaneous adipose tissue.

Beige adipocytes may be embedded in white adipose tissue and can produce heat by the increase in the number and function of mitochondria and UCP-1 expression (33, 34). A variety of stimuli can induce this response, such as exercise-induced muscle production of irisin (35) or dietary components (36). Cold exposure also influences the development of beige adipocytes by increasing the sympathetic tone by the production of catecholamines (37). CRF combines cold and heat by cooling the body surface and heating the inner layers of the dermis, including subcutaneous fat depots. In this study, we showed that CRF application after 0, 3, 6 and 12 h change the morphology of adipose tissue partially into those adipocytes similar to beige, especially in the inguinal adipose tissue. After 7 d of CRF application, this alteration remained, and the expression of UCP-1 increased in inguinal adipose tissue. Koh et al. (2018) demonstrated in a model of diet-induced obesity that three weeks after radiofrequency applications, increased UCP-1 expression and beige adipocyte presence in the adipose tissue (25). We demonstrated that only one application of CRF induces beige adipocytes, demonstrating the rapid capacity of this therapy to produce beige adipocytes and consequently stimulate thermogenesis.

Strategies that aim for the development of beige adipocytes are in focus and one of the reasons is the increase in mitochondria that promotes higher energy expenditure in white adipose tissue (38, 39). In this case, browning of adipose tissue is considered a way of treating obesity since increased energy expenditure promotes the reduction of adipose tissue mass and, consequently, weight loss (36, 38, 40). The essential limitation of this study is the number of applications, and thus, a short period of adipose tissue observation; it was not possible to demonstrate the effect of CRF on obesity over the long-term. However, we believe that our data show that CRF may also have the potential to be a strategy to reduce localized fat deposits as a new therapy to induce beige adipocyte formation.

Therefore, we demonstrated that the application of CRF effectively changes adipose tissue morphology while increasing the formation of beige adipocytes with higher expression of UCP-1. These alterations may indicate that CRF therapy can contribute to the development of adipocytes prone to thermogenesis, which is a new option to increase energy expenditure and, consequently, reduce localized fat pad.

Acknowledgments: The research team would like to thank Andreia Almeida and Body Health Brazil for providing the CRF device and technical assistance for this study.

REFERENCES

1. Choe SS, Huh JY, Hwang IJ, Kim JI & Kim JB (2016) *Front Endocrinol (Lausanne)* **7**, 30.
2. Virtanen KA, Lidell ME, Orava J, Heglind M, Westergren R, Niemi T, Taittonen M, Laine J, Savisto NJ, Enerback S & Nuutila P (2009) *N Engl J Med* **360**, 1518-1525.
3. Feldmann H M, Golozoubova V, Cannon B & Nedergaard J (2009) *Cell Metab* **9**, 203-209.
4. Shabalina I G, Petrovic N, de Jong JM, Kalinovich AV, Cannon B & Nedergaard J (2013) *Cell Rep* **5**, 1196-1203.
5. Ikeda K, Maretich P & Kajimura S (2018) *Trends Endocrinol Metab* **29**, 191-200.

6. Shin W, Okamatsu-Ogura Y, Matsuoka S, Tsubota A & Kimura K (2019) *J Vet Med Sci* **81**, 799-807.
7. Makki K Froguel P & Wolowczuk I (2013) *ISRN Inflamm* **2013**, 139239.
8. Reilly JJ, El-Hamdouchi A, Diouf A, Monyeki A & Somda SA (2018) *Lancet* **391**, 1773-1774.
9. Hall KD & Guo J (2017) *Gastroenterology* **152**, 1718-1727 e1713.
10. Benatti FB, Lira FS, Oyama LM, do Nascimento CM & Lancha Jr H (2011) *Diabetes Metab Syndr Obes* **4**, 141-154.
11. Ingargiola MJ, Motakef S, Chung MT, Vasconez HC & Sasaki GH (2015) *Plast Reconstr Surg* **135**, 1581-1590.
12. Chia CT, Neinstein RM & Theodorou SJ (2017) *Plast Reconstr Surg* **139**, 267e-274e.
13. Suh DH, Kim CM, Lee SJ, Kim H, Yeom S K & Ryu HJ (2017) *J Cosmet Laser Ther* **19**, 89-92.
14. Hayre N, Palm M & Jenkin P (2016) *J Drugs Dermatol* **15**, 1557-1561.
15. Wanitphakdeedecha R, Sathaworawong A, Manuskiatti W & Sadick NS (2017) *J Cosmet Laser Ther* **19**, 205-209.
16. Pumprla J, Howorka K, Kolackova Z & Sovova E (2015) *F1000Res* **4**, 49.
17. Adatto MA, Adatto-Neilson RM & Morren G (2014) *Lasers Med Sci* **29**, 1627-1631.
18. Boisnic S, Divaris M, Nelson AA, Gharavi NM & Lask GP (2014) *Lasers Surg Med* **46**, 94-103.
19. Vale AL, Pereira AS, Morais A, Noites A, Mendonca AC, Martins Pinto J, Vilarinho R & Carvalho P (2018) *J Cosmet Dermatol* **17**, 703-711.
20. Vilela MC, Mansur DS, Lacerda-Queiroz N, Rodrigues DH, Arantes RM, Kroon EG, Campos MA, Teixeira MM & Teixeira AL (2008) *Neurosci Lett* **445**, 18-22.
21. Oliveira AB, Moura CF, Gomes-Filho E, Marco CA, Urban L & Miranda MR (2013) *PLoS One* **8**, e56354.
22. Souza DG, Soares AC, Pinho V, Torloni H, Reis LF, Teixeira MM & Dias AA (2002) *Am J Pathol* **160**, 1755-1765.
23. Barcelos LS, Talvani A, Teixeira AS, Cassali GD, Andrade SP & Teixeira MM (2004) *Inflamm Res* **53**, 576-584.
24. Qiu Y, Nguyen KD., Odegaard JI, Cui X, Tian X, Locksley RM, Palmiter RD & Chawla A (2014) *Cell* **157**, 1292-1308.
25. Koh YJ, Lee JH & Park SY (2018) *Evid Based Complement Alternat Med* **2018**, 4737515.
26. Jensen MD (2008) *J Clin Endocrinol Metab* **93**, S57-63.
27. Dierickx CC (2006) *Lasers Surg Med* **38**, 799-807.
28. Dinno MA, Dyson M, Young SR, Mortimer AJ, Hart J & Crum LA (1989) *Phys Med Biol* **34**, 1543-1552.
29. Brown SA, Greenbaum L, Shtukmaster S, Zadok Y, Ben-Ezra S & Kushkuley L (2009) *Plast Reconstr Surg* **124**, 92-101.
30. Widgerow AD, Kilmer SL, Garruto JA & Stevens WG (2019) *J Drugs Dermatol* **18**, 375-380.
31. Pereira JX, Cavalcante Y & Wanzeler de Oliveira R (2017) *Clin Cosmet Investig Dermatol* **10**, 57-66.
32. McDaniel D, Fritz K, Machovcova A & Bernardy J (2014) *J Drugs Dermatol* **13**, 1336-1340.
33. Bartelt A & Heeren J (2014) *Nat Rev Endocrinol* **10**, 24-36.
34. Enerback S, Jacobsson A, Simpson EM, Guerra C, Yamashita H, Harper ME & Kozak LP (1997) *Nature* **387**, 90-94.
35. Bostrom P, Wu J, Jedrychowski MP, Korde A, Ye L, Lo JC, Rasbach KA, Bostrom EA, Choi JH, Long JZ, Kajimura S, Zingaretti MC, Vind BF, Tu H, Cinti S, Hojlund K, Gygi SP & Spiegelman BM. (2012) *Nature* **481**, 463-468.
36. Baskaran P., Krishnan V, Ren J & Thyagarajan B (2016) *Br J Pharmacol* **173**, 2369-2389.
37. Fisher F M, Kleiner S, Douris N, Fox, EC, Mepani RJ, Verdeguer F, Wu J, Kharitonenkov A, Flier JS, Maratos-Flier E & Spiegelman BM (2012) *Genes Dev* **26**, 271-281.
38. Harms M & Seale P (2013) *Nat Med* **19**, 1252-1263.
39. Kopecky J, Clarke G, Enerback S, Spiegelman B & Kozak LP (1995) *J Clin Invest* **96**, 2914-2923.
40. Xing T, Kang Y, Xu X, Wang B, Du M & Zhu MJ (2018) *Mol Nutr Food Res* **62**, 1701035.